Fuel Processing Technology 129 (2015) 67–74

Contents lists available at ScienceDirect

Fuel Processing Technology

journal homepage: www.elsevier.com/locate/fuproc

Thermogravimetric analysis of the combustion of dry distiller's grains with solubles (DDGS) and pyrolysis char under kinetic control

Carmen Branca [a],*, Colomba Di Blasi [b]

[a] Istituto di Ricerche sulla Combustione, C.N.R., P.le V. Tecchio, 80125 Napoli, Italy
[b] Dipartimento di Ingegneria Chimica, dei Materiali e della Produzione Industriale, Università degli Studi di Napoli "Federico II", P.le V. Tecchio, 80125 Napoli, Italy

ARTICLE INFO

Article history:
Received 18 June 2014
Received in revised form 6 August 2014
Accepted 23 August 2014
Available online 16 September 2014

Keywords:
DDGS
Combustion
Kinetics
Reactivity

ABSTRACT

The combustion behavior of dry distiller's grains with solubles (DDGS) and the corresponding pyrolysis char using a thermogravimetric system is studied. Comparison with beech wood indicates that DDGS devolatilization occurs with a slower rate and the char consists of two fractions with different reactivity. Thermogravimetric curves, obtained with heating rates between 2.5 and 20 K/min, are used to develop a multi-step global reaction mechanism. The description of DDGS devolatilization requires four reactions, representative of the evolution of lumped classes of components, with activation energies of 95, 107, 106 and 100 kJ/mol, which are lower than those typically associated with wood devolatilization. DDGS char combustion is well described by two reaction steps with activation energies of 137 and 153 kJ/mol that again barely touch the lower limit of the typical range of values reported for lignocellulosic chars.

© 2014 Elsevier B.V. All rights reserved.

1. Introduction

Apart from sugars directly fermentable, the main source of ethanol is currently starch from corn, wheat and barley. Enzymatic hydrolysis is applied to transform starch into sugars which are then fermented by yeasts to produce ethanol, corresponding to about 50% of the grain's energy [1]. The solid residues of this process are indicated as dry distiller's grains with solubles (DDGS). For a dry-grind process [2], the whole stillage (water and solids remaining after distillation of ethanol, comprised primarily of water, fiber, protein, and fat) is centrifuged to separate coarse solids from liquid. The liquid, called thin stillage, goes through an evaporator to remove additional moisture resulting in condensed distiller's solubles (syrup) which contain approximately 30% dry matter. Condensed distiller's solubles, combined with the coarse solids fraction and dried, give rise to DDGS. This residue contains mainly proteins, cellulose, hemicellulose and lignin from the original cereal, with the addition of residual starch and yeast [3]. It is mainly used as a source of protein and energy for ruminants but its increasing production in recent years has motivated the search of alternative uses such as thermal and chemical conversion for bio-energy and bio-fuels. Therefore, for an efficient exploitation, thermo-chemical characterization is needed.

Thermogravimetric analysis, based on integral (TG) and differential data (DTG), is widely recognized as an excellent means to examine the chief characteristics of the conversion process under a controlled environment and is often associated with kinetic modeling. In particular the heterogeneous reaction rates of biomass and char conversion are needed to formulate both empirical rules and kinetic mechanisms that should be coupled with the mathematical description of heat, mass and momentum transfer, to provide advanced tools for combustor/gasifier design and optimization. Therefore, the intrinsic rate, that is, the rate of the reaction step free from heat and mass transfer limitations should be investigated [4]. On the other hand, in commercial thermogravimetric systems the sample temperature is not directly measured or controlled, so that the high exothermicity of the combustion reactions may result in significant deviations between the programmed and the actual sample temperature [5–7]. Moreover a shift from kinetic to diffusion control occurs when the temperature, the heating rate, the sample mass and/or the particle sizes are increased above certain limits [4]. Although numerous studies have been made to investigate the thermogravimetric behavior of biomass under oxidative conditions, kinetic models have been developed only in a relatively few cases [8–21], which can be considered potentially correct. Indeed, they are based on measurements carried out at different heating rates with multiple curve evaluation leading to invariant kinetic parameters. This approach has not yet been applied for DDGS combustion which has until now received scarce consideration.

DDGS thermogravimetric curves in inert atmosphere show three distinct peaks [22–24], in addition to that caused by moisture evaporation, and the attainment of char yields around 20–25%. In air, the devolatilization stage is followed by char combustion [25,26]. Moreover, the dynamic TGA analysis of DDGS char in oxidizing environment at moderate heating rates [23,27] indicates a multi-step process. Devolatilization kinetics in inert atmosphere are described using multiple experiments by means of a distributed activation energy method (25 parallel first order reactions) [22] or using a single experiment

---

* Corresponding author. Tel.: +39 081 7682232; fax: +39 081 5936936.
E-mail address: branca@irc.cnr.it (C. Branca).

http://dx.doi.org/10.1016/j.fuproc.2014.08.019
0378-3820/© 2014 Elsevier B.V. All rights reserved.

modeled with two global reactions [23]. Global one-step combustion kinetics is proposed in Ref. [26] for the sequential devolatilization of DDGS and combustion of char with parameters dependent on the heating rate and thus not representative of intrinsic kinetics. Moreover a single experiment is used in Ref. [23] to model char combustion. Instead both isothermal and dynamic data of DDGS char combustion, obtained by varying heating rate and final temperature, are used in Ref. [27]. Unfortunately, however, some of the measurements show incongruities most likely as a consequence of serious mass (oxygen) transfer limitations and probably thermal runaway, due to the rather severe thermal conditions employed, so also affecting the results of the kinetic analysis.

The brief analysis of the state of the art shows that, although mechanisms representative of the intrinsic kinetics of heterogeneous combustion are available for lignocellulosic fuels and a unified treatment has been recently proposed [20], accurate kinetic models are not available for DDGS combustion. Accurate kinetic mechanisms are needed for incorporation into advanced models aimed at optimizing practical conversion systems and also for improving the understanding of experimental results generally obtained from chemical reactors dominated by heat and mass transfer, such as for instance, for various thermochemical processes [1,28–32]. In this study, thermogravimetric curves are measured by means of a previously developed system, which permits precise measurement and control of the sample temperature. Moreover not only the reactions take place under exactly known thermal conditions but also the sample mass and particle sizes are accurately determined so as there is no limitation from the rate of oxygen diffusion. Measurements are made for both DDGS and DDGS char samples in air by varying the heating rate. The TG and DTG data are used to formulate a kinetic mechanism with the evaluation of the related parameters. Previous results obtained for beech wood samples are used for comparison.

2. Materials and methods

2.1. Materials

The DDGS sample has been provided in the framework of the European project BRISK from the same batch previously used [22], obtained by the company Abengoa from a plant in Spain converting barley seeds (Hordeum Vulgare) into ethanol with a dry-grind process. The elemental composition of the sample, listed in Table 1, is also that previously reported [22]. For comparison purposes, beech wood data are also enclosed. The C and H contents of DDGS are comparable to those of wood but the N and S contents are higher. The reported ash content of 7.1% [22] is also much higher than that of beech wood (around 0.4% [33]). According to literature [23], the DDGS ash contains large quantities of P, K, Na and Mg that imply a fouling tendency and also a possible catalytic action on the reaction rates.

In general, there is not agreement in relation to the chemical composition of DDGS which is scarcely investigated, although it highly affects the conversion rate. It can be expected that it is in same way dependent on the origin fuel and the conversion process. According to [34], corn-originated DDGS composition consists of: water extractives 24.7%, ether extractives 11.6%, crude protein 24.9%, glucan (cellulose and starch) 21.2%, xylan and arabinan 13.5%, and ash 4.5% (dry matter 88.8%). Instead for the wheat-originated DDGS [23] a total contribution of the main biomass components around 33% is reported (hemicellulose, about 22%, is the most abundant because harder to ferment compared to cellulose, 7.6% cellulose and 2.88% lignin) with a protein content around 10%.

Table 1
Elemental composition of the DDGS and DDGS char samples (data for beech wood and beech wood char are also included for comparison; oxygen by difference).

	DDGS	Beech wood	DDGS char	Beech wood char
C	49	48.3	59.3	78
H	6.3	6.02	2.64	3.2
N	4.5	0.30	6.20	0.25
S	0.4	<0.05	n.a.	n.a.
O	39.8	45.3	31.9	18.6

Table 1 also lists the ultimate analysis of DDGS and beech wood char samples obtained at a pyrolysis temperature of 800 K following the procedure described below. Apart from the obvious increase in the C content for both cases with respect to the origin fuels, it can be noticed that a lower value is shown by the DDGS char.

2.2. Experimental details

Two different sets of tests are carried out with the scope of investigating 1) the thermogravimetric behavior of DDGS and DDGS char combustion and producing weight loss curves to be used for kinetic analysis and 2) the morphological structure of char produced from DDGS pyrolysis, studied by means of Scanning Electron Microscope (SEM), and the char samples to be used for the thermogravimetric tests. The first set of experiments is made in air using DDGS or DDGS char pellets previously milled to powder (particle sizes below 80 μm) and pre-dried for 10 h at 373 K. The second set of experiments is made in nitrogen using single DDGS pellets with no pretreatment apart from pre-drying as above.

The thermogravimetric tests are made using a non-commercial system already extensively applied to study solid conversion under conditions of kinetic control [8,11,20,21,35–40], where the pulverized sample is settled in the shape of a layer extending over a surface of 4 mm × 20 mm and exposed to a nominal air velocity of 30 mm/s. The temperature of the sample layer, whose thickness is the characteristic size of the process, is measured, by a close-coupled thin thermocouple, and controlled using the intensity of the applied radiative heat flux as the adjustable variable. In this way it is possible to carry out the tests under exactly determined thermal conditions of the sample. For both DDGS and DDGS char, it has been observed that sample layer thicknesses up to 150 μm allow a good temperature control to be achieved and avoid heat and mass transfer limitations. In fact, given maximum heating rates of 40 K/min and a final temperature of 950 K, thermogravimetric curves remain unchanged when the layer thickness is further reduced. Hence, the tests are made for sample layers about 110 μm thick (5 mg mass) using a final temperature of 950 K and heating rates of 2.5–20 K/min (2.5, 5, 10 and 20 K/min for DDGS; 5, 10 and 15 K/min for DDGS char). Each thermogravimetric test is made in triplicate, showing good repeatability (maximum deviations between the measured weight loss curves are always in the range 0.1–0.3%).

The second set of experiments is carried out for the pyrolysis of single DDGS pellets (length 20 mm and diameter 6 mm), instantaneously suspended in a pre-heated (isothermal) cylindrical stainless reactor [36,40] at the temperature of 800 K. Each pyrolysis test is made in triplicate, showing an excellent reproducibility in relation to the char yield (standard deviation of 0.1%). Good reproducibility is also obtained for the time profile of the pellet center temperature with maximum deviations of ± 2 K. The same deviations are also observed for beech wood pellets, of the same size and subjected to pre-drying as the DDGS pellets, used for comparison. The center pellet temperature profile is the same for both DDGS and beech wood at low temperatures (below 600 K). However, during the reaction period, the temperature dynamics of beech wood pellets are clearly affected by reaction heat effects as already discussed in the previous work [41]. Instead, for DDGS, the shape of the temperature profile does not bring any evidence directly related to exothermicity during pyrolysis. As expected, the final temperature reached by the two char samples is the same (about 20 K below the heating temperature). Finally, the DDGS char yield is 27 wt.% (versus 20% of beech wood).

3. Results

The main characteristics shown by the thermogravimetric curves are discussed and used to formulate a multi-step combustion mechanism. Then the related kinetic constants are estimated.

3.1. Thermogravimetric behavior and morphological structure of char

The main features of the thermogravimetric curves for DDGS and DDGS char combustion can be seen from Fig. 1A and B (heating rate 5 K/min) where, for comparison purposes, the data obtained for beech wood and beech wood char are also plotted. Moreover to facilitate the comparison between the results of this study and those already available in the literature, also in relation to pyrolysis conditions, the differential thermogravimetric curves obtained for a heating rate of 10 K/min are reported in Fig. 1C together with those for as-received DDGS in nitrogen and DDGS char in air adapted from Ref. [22] and Ref. [27], respectively. The selection of these two specific curves is justified by the use of samples of similar properties with those of the present study.

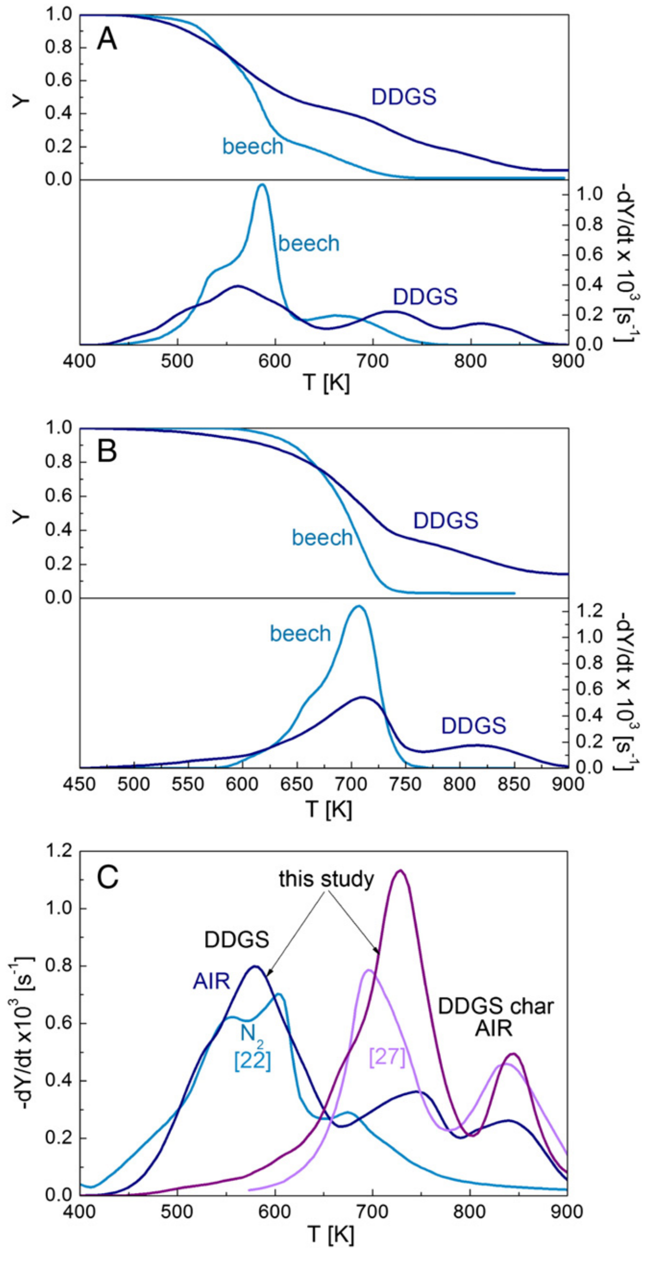

Fig. 1. A–C — mass fraction, Y, and mass loss rate, −dY/dt, for DDGS and beech wood (A) and the corresponding chars (produced from single pellets pyrolysis at 800 K) (B) in air versus temperature (heating rate 5 K/min); mass loss rate for DDGS and the corresponding char in air and for DDGS in nitrogen [22] and DDGS char in air [27] versus temperature (heating rate 10 K/min) (C).

The separation between the devolatilization and the char oxidation zones, which is well evident for beech wood, is not immediately identifiable for DDGS, owing to the much wider temperature interval where the processes of interest take place and the more complex shape of the rate curves (Fig. 1A). As shown by the DDGS curve reported in Fig. 1C [22] and also found in other cases [23,24], in inert environment, a first reaction zone appears where the large part of the volatile products are released, followed at higher temperature (above 623–673 K) by a further zone of slower devolatilization rate. Two peaks/shoulders are identified for the first zone around 553–573 K and 603 K [22–24] whereas the second zone presents another visible peak around 673–723 K [22,24] or slowly decreasing rates [23]. The differences, among the various studies, are due to different experimental systems/conditions and the different nature and conditions of the feedstock.

Apart from very low temperatures (below 500 K), where the differences in the mass loss rate can be attributed to the different initial moisture contents (as-received and pre-dried sample for nitrogen and air, respectively), the DDGS curves obtained in nitrogen [22] and air reported in Fig. 1C show significant similarities. In air a first zone of intense devolatilization is also observed, delimited by a temperature of around 650 K and a solid mass fraction of about 0.40, with two peaks positioned at about 520 and 570 K, respectively. The peak rates are anticipated at slightly lower temperatures and there is overlap as a consequence of the enhancement in the degradation process caused by the presence of oxygen, as already observed for lignocellulosic fuels [15].

After a local minimum, the main features of the second zone, in the presence of air, at higher temperature, consist of two well defined peaks at about 730 and 839 K (heating rate 5 K/min) which are also exhibited by the DDGS char investigated in separate experiments (Fig. 1B, C). The two-stage feature of DDGS char oxidation is also reported by previous studies with peaks around 700–750 K and 850 K [23,27] (see also Fig. 1C). Again the quantitative discrepancies between the results of this study and previous findings can be attributed to the difference in the experimental conditions, during pyrolysis and combustion, and the sample properties. In particular, the first zone of char combustion (Fig. 1C) is largely dependent on the pyrolysis conditions which, among others, determine the total volatile content of the samples. From the comparison between the curves obtained from DDGS and corresponding char it can be inferred that, while in the absence of oxygen the third peak [22,24] (Fig. 1C) or the flat zone [23] of the DDGS curve is small as it is associated with small amounts of released mass; devolatilization and oxidation take place simultaneously in oxidizing environments, thus justifying the higher rates and especially the higher peaks. Although the first zone of intense devolatilization is more or less localized over the same temperature range as for beech wood, the DDGS rates of volatile release are much lower as, in the absence of oxygen, the devolatilization process would slowly continue at higher temperature. In air, simultaneously to devolatilization, the heterogeneous reactions of char combustion also begin, so that, contrary to wood, the overlap between the two processes is much more intense. Moreover, while the kinetic analysis of the devolatilization stage of beech wood [20] leads to clearly identify the contribution of the main components, this task is more difficult for DDGS. The peak rates observed from previous thermogravimetric measurements carried out in nitrogen are attributed to the main components of lignocellulosic biomass but the percentage of cellulose and lignin in the actual DDGS chemical composition is generally small. In addition to the usual products of lignocellulosic biomass degradation, at higher temperature (second zone of the devolatilization stage) the release is also observed [23] of few long chain fatty acids and heterocyclic aromatics like indole and pyrrole, generally identified as pyrolysis products of amino acids. Indeed one of the chief differences between DDGS and lignocellulosic biomass is due to the significant content of proteins whose model compounds are reported [3] to mainly degrade at temperatures close to 573 K. However, depending on their specific nature, degradation temperatures as low as 500 K and as high as 708 K may also be attained. Also, the analysis [23] shows that DDGS in inert environment loses some mass between 473 and 523 K, attributed to the evaporation/decomposition of oils like glycerine, palmitic acid and linoleic acid. Therefore it is likely that the different reaction zones shown by the thermogravimetric curves are associated with the simultaneous decomposition of various chemical components. On the other hand, for the zone of intense devolatilization, although a shoulder and a peak are also shown by the DDGS sample, their positions are shifted at lower temperatures with respect to beech wood. It can be hypothesized that the large amounts of ashes present in DDGS may also play a role in this matter, as it is known that alkali metals displace thermal degradation at lower temperatures [42].

Apart from the overlap with the devolatilization reactions at low temperatures, compared with beech wood char, the oxidation of DDGS char begins at slightly higher temperatures. Moreover, instead of the single well defined reaction zone generally observed for lignocellulosic chars, it presents two distinct zones with especially the second one evolving at much higher temperatures. This peculiar behavior is explained by the possible existence of two types of chars generated from different parts of the initial fuel consisting of distiller's grains and concentrated distiller's solubles [23]. Furthermore the morphological structure does not reproduce that typical of wood [39], resulting in pores of different sizes and shape and the presence of some deposits as shown by the SEM images in Fig. 2A–B and already reported [27]. Despite of the grinding process, it can also be seen, through Fig. 2C–D that the char may partially retain the original structure of the de-hulled barley seeds (consisting of the external aleurone layer (bran), made of proteins and fibers and amounting to about 15%, the starchy endosperm cells containing big and small starch granules surrounded by the protein matrix and corresponding to about 85%, and the germ (embryo) made of proteins and lipids for about 2% [43,44]). More specifically the porous structure resembles that of the protein matrix of the endosperm and the aleurone layer empty of the starch granules, as a consequence of their previous exploitation for ethanol production.

The main features of the thermogravimetric curves measured for DDGS and DDGS char remain qualitatively the same as the heating rate is varied in the range 2.5–20 K/min. However, as already observed for wood and agricultural residues [15,20], as the heating rate is increased, the reactions tend to occur at higher temperatures and the overlapping between the various reaction zones is enhanced.

3.2. Combustion kinetics

Kinetic models of biomass devolatilization generally assume that volatiles are released according to a set of parallel reactions for the lumped components that, in air, are associated with a further set of one or two heterogeneous reactions for the combustion of char [4–6, 9–21]. Parallel reaction models are generally preferred to sequential

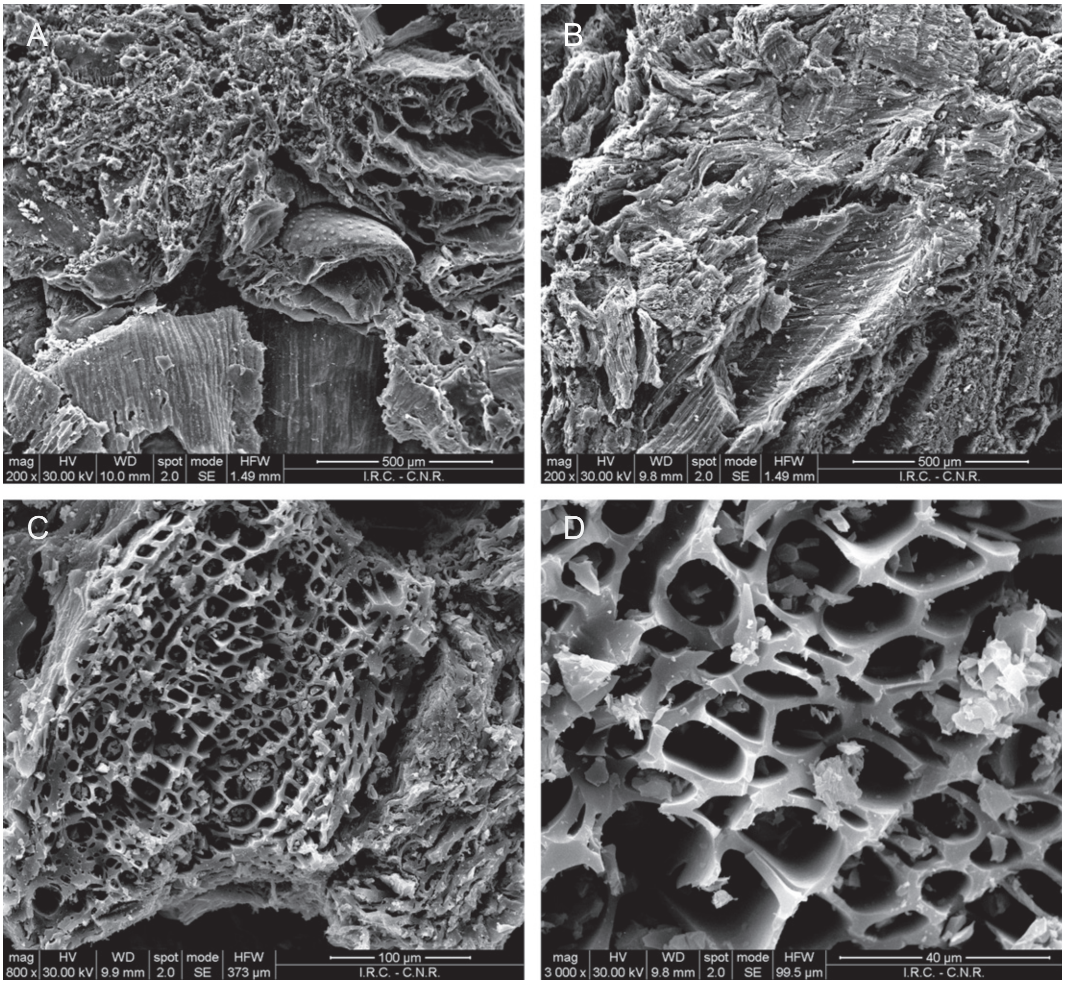
A
mag | HV | WD | spot | mode | HFW | 500 µm
200 x | 30.00 kV | 10.0 mm | 2.0 | SE | 1.49 mm | I.R.C. - C.N.R.
B
mag | HV | WD | spot | mode | HFW | 500 µm
200 x | 30.00 kV | 9.8 mm | 2.0 | SE | 1.49 mm | I.R.C. - C.N.R.
C
mag | HV | WD | spot | mode | HFW | 100 µm
800 x | 30.00 kV | 9.9 mm | 2.0 | SE | 373 µm | I.R.C. - C.N.R.
D
mag | HV | WD | spot | mode | HFW | 40 µm
3 000 x | 30.00 kV | 9.8 mm | 2.0 | SE | 99.5 µm | I.R.C. - C.N.R.

Fig. 2. A–C — SEM images of the char produced from the isothermal pyrolysis of single DDGS pellets at 800 K at various magnifications.

reaction models, owing to the higher flexibility provided by the estimation of appropriate set of parameter values which permit overlaps between reaction zones. In this way both parallel and series processes can be well described with the chief kinetic parameters remaining practically unaltered [45]. Therefore, a set of N independent parallel reactions for lumped components is also assumed to describe both stages for DDGS:

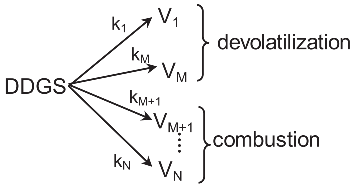

(a_1)

(a_M)

(a_{M+1})

(a_N)

with the formation of the lumped volatile products V_i ($i = 1,\ldots,N$). From the chemical point of view, reactions $a_1,\ldots,a_M$ are associated with solid devolatilization, and reactions $a_{M+1},\ldots,a_N$ are associated with char combustion.

The dependence of the reaction rates on temperature is expressed by the Arrhenius law (A_i is the pre-exponential factor and E_i is the activation energy), whereas the evolution of the pore surface area during conversion is taken into account by a power law dependence (exponent n_i) on the solid mass fraction [4]. The component dynamics are described by N ordinary differential equations written for the mass fractions, Y_i, of the reacting solid fuel:

$$\frac{dY_i}{dt} = A_i \exp\left(-\frac{E_i}{RT}\right) Y_i^{n_i}; Y_i(0) = \nu_i, i = 1, n \tag{1–2}$$

where the temperature, T, is a known function of time.

The kinetic parameters to be estimated are: A_i, E_i, n_i and ν_i (the latter are usually indicated as stoichiometric coefficients). Also, the numbers of devolatilization (M) and combustion (N–M) reactions, strictly required for an accurate description of the experimental data, are also model parameters to be evaluated. The parameters are numerically estimated considering simultaneously both TG and DTG data for the various heating rates, following the method already described [36].

The estimated parameters are invariant with the heating rate, except for the stoichiometric coefficients which are allowed to show small variations owing to the influence of the thermal conditions on the volatile yields. Finally deviations between measurements and model predictions, dev_{TG} and dev_{DTG}, are defined as in [32].

The application of the optimization procedure to the integral and differential curves reveals that, for the DDGS char samples, a good description of the process requires two steps for the low-temperature zone and two further steps for the description of the peak rates, giving $N = 4$ and $M = 2$. In addition to the two steps needed to describe the oxidation of char, four additional reaction steps should be considered for the devolatilization stage of DDGS, resulting in $N = 6$ and $M = 4$. Also, the activation energies of the four-step reaction mechanism of DDGS char combustion are the same as those of the corresponding steps of the DDGS combustion mechanism. Small variations on the other parameters are allowed to take into account the effects associated with the different thermal condition of char formation. The estimated values of the kinetic parameters and the deviations between predictions and measurements for the combustion of DDGS and DDGS char are reported in Tables 2–3. Examples of the component dynamics are shown in Fig. 3 (DDGS) and Fig. 4 (DDGS char) for a heating rate of 5 K/min. The agreement between predictions and measurements is good as indicated by the small values of the deviations (Tables 2–3) and the comparison between global rates of mass loss made in Figs. 5–6 for the various heating rates and the two samples. Furthermore, thermogravimetric curves, for both DDGS and DDGS char, have also been re-evaluated using constant

Table 2

Estimated kinetic parameters (activation energy, E, pre-exponential factor, A, reaction order, n, and stoichiometric coefficient, ν) for the combustion of DDGS and corresponding deviations between measured and simulated integral (dev_{TG}) and differential (dev_{DTG}) curves (the parameters are invariant with the heating rate, h, except for small variations on the stoichiometric coefficients; deviations are also provided when constant (average) values of the stoichiometric coefficients are used).

Parameter	DDGS
E_1 [kJ/mol]	94.7
A_1 [s^{-1}]	3.46×10^7
n_1	1.20
E_2 [kJ/mol]	107.2
A_2 [s^{-1}]	4.93×10^7
n_2	1.10
E_3 [kJ/mol]	105.9
A_3 [s^{-1}]	5.31×10^6
n_3	1.00
E_4 [kJ/mol]	100.1
A_4 [s^{-1}]	2.01×10^5
n_4	0.95
E_5 [kJ/mol]	136.6
A_5 [s^{-1}]	2.05×10^7
n_5	0.98
E_6 [kJ/mol]	152.8
A_6 [s^{-1}]	1.94×10^7
n_6	1.15

h [K/min]								
Parameter	2.5	5	10	20	2.5	5	10	20
ν_1	0.07	0.10	0.110	0.120	0.10			
ν_2	0.21	0.21	0.230	0.230	0.22			
ν_3	0.23	0.20	0.19	0.18	0.20			
ν_4	0.07	0.07	0.08	0.08	0.075			
ν_5	0.19	0.19	0.160	0.160	0.175			
ν_6	0.175	0.175	0.175	0.175	0.175			
dev_{TG} [%]	0.67	0.40	0.26	1.08	1.94	0.46	0.71	1.83
dev_{DTG} [%]	2.64	2.13	1.25	2.64	5.34	2.93	1.90	3.57

Table 3
Estimated kinetic parameters (activation energy, E, pre-exponential factor, A, reaction order, n, and stoichiometric coefficient, ν) for the combustion of DDGS char and corresponding deviations between measured and simulated integral (dev_{TG}) and differential (dev_{DTG}) curves (the parameters are invariant with the heating rate, h, except for small variations on the stoichiometric coefficients; deviations are also provided when constant (average) values of the stoichiometric coefficients are used).

Parameter	Char DDGS
E_1 [kJ/mol]	105.9
A_1 [s^{-1}]	3.00×10^7
n_1	1.20
E_2 [kJ/mol]	100.1
A_2 [s^{-1}]	3.80×10^5
n_2	0.95
E_3 [kJ/mol]	136.6
A_3 [s^{-1}]	1.82×10^7
n_3	0.98
E_4 [kJ/mol]	152.8
A_4 [s^{-1}]	1.0×10^7
n_4	1.15

h [K/min]						
Parameter	5	10	20	5	10	20
ν_1	0.04	0.03	0.02	0.03		
ν_2	0.11	0.10	0.10	0.10		
ν_3	0.49	0.48	0.47	0.48		
ν_4	0.22	0.25	0.27	0.25		
dev_{TG} [%]	0.46	0.76	0.71	1.05	0.76	0.30
dev_{DTG} [%]	1.82	3.25	1.67	2.49	3.25	1.70

(average) stoichiometric coefficients and the values already estimated for the other parameters. As expected and confirmed by the results reported in Tables 2–3, the deviations increase (especially for the minimum and maximum heating rates) but remain small. Therefore, constant stoichiometric coefficients can be safely used when incorporating this kinetic mechanism into transport models.

Fig. 3 shows that the four reactions, describing DDGS devolatilization, evolve over a temperature range of about 400–710 K with significant overlap. This indicates that they are global reactions actually taking into account the evolution of several chemical components. This circumstance is also confirmed by the relatively low values of the estimated activation energies (95, 107, 106 and 100 kJ/mol). Indeed these are significantly lower than those typically reported for the devolatilization of the pseudo-components hemicellulose, cellulose and lignin for lignocellulosic materials, as a result of a simultaneous evaluation of at least three experiments conducted under different thermal conditions (for instance, values of 147, 200 and 173 kJ/mol for beech wood [20]). Apart from the very low contents of hemicellulose, cellulose and lignin in the DDGS sample, it appears that classes of protein components and extractives and starch do not degrade over narrow well defined temperature ranges. This is not unexpected given the significant number of components which present different reactivity [3]. The large amount of ash and the presence of species catalytically active also participate to widen the range of the reaction temperatures. Reaction steps 2 and 3 are quantitatively the most important contributing for approximately 22 and 20% of the total mass released. The reaction steps 1 and 4 approximately cause the further release of about 8 and 10% mass, respectively. The amounts of volatiles released during the slow devolatilization of the char sample at low (below 650 K) temperature (Fig. 4) are relatively small (about 3 and 10% of the total mass). The presence of this residual volatile matter can be attributed to the mild thermal conditions employed during pyrolysis.

As expected, the dynamics of the two components describing the combustion of char are qualitatively the same for the two samples (Figs. 3–4). The two global reactions present activation energies of 137 and 153 kJ/mol which barely touch the lower limit of the range of values

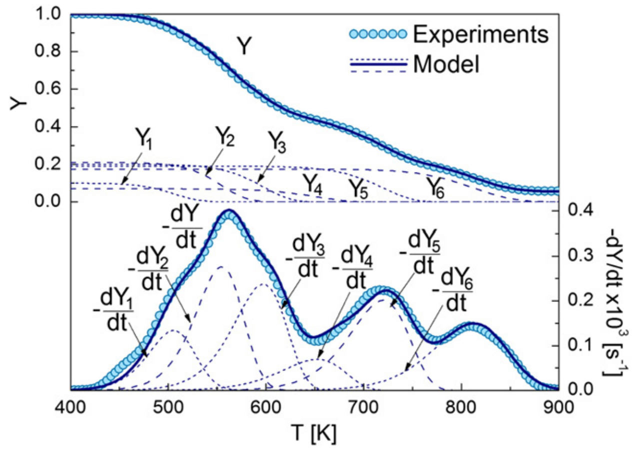

Fig. 3. Comparison between the measured (symbols) and the simulated (solid lined) mass fraction and rate of mass loss for the DDGS sample in air with heating rate, h, of 5 K/min up to 950 K. Thin lines with various styles denote the predicted evolution of the mass fraction and rate of mass loss for the various reaction zones: 1, 2, 3, 4 devolatilization of the DDGS; 5, 6 combustion of char (kinetic parameters listed in Table 2).

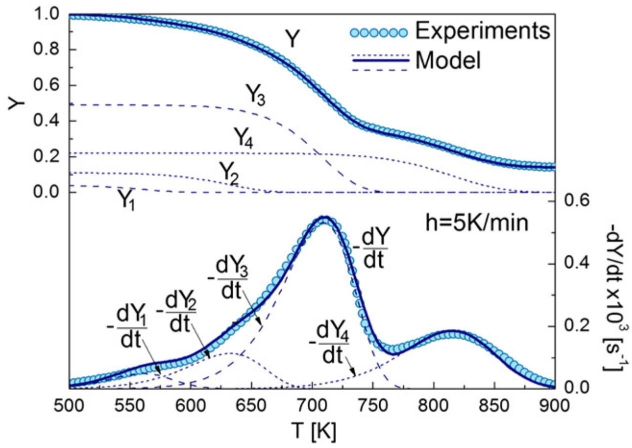

Fig. 4. Comparison between the measured (symbols) and the simulated (solid lined) mass fraction and rate of mass loss for the DDGS char sample (produced from single pellets pyrolysis at 800 K) in air with heating rate, h, of 5 K/min up to 950 K. Thin lines with various styles denote the predicted evolution of the mass fraction and rate of mass loss for the various reaction zones: 1, 2 devolatilization; 3, 4 combustion of char (kinetic parameters listed in Table 3).

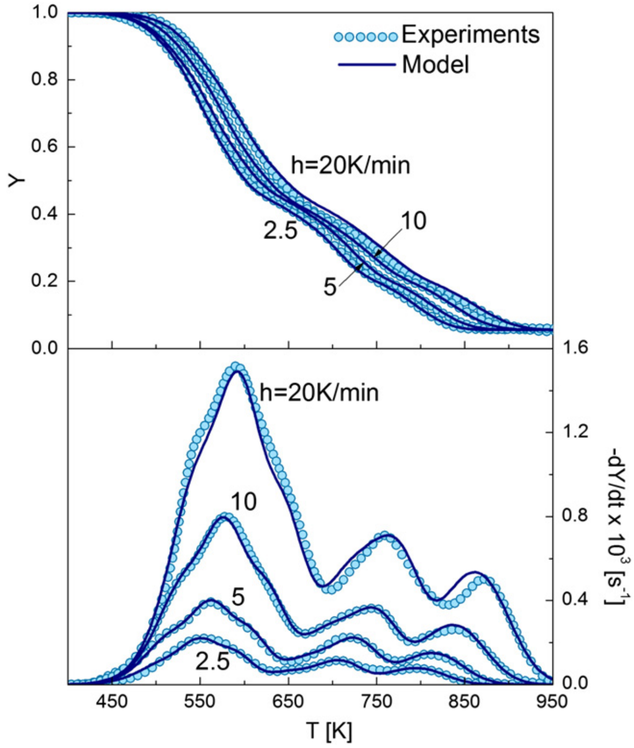

Fig. 5. Comparison between measured (symbols) and simulated (solid lines) thermogravimetric curves for the DDGS samples at various heating rates, h, in air up to a temperature 950 K (kinetic parameters listed in Table 2).

reported for lignocellulosic chars (140–230 kJ/mol [4]) when the devolatilization stage is adequately taken into account. It is plausible that the peculiar composition of the origin material as well as its morphological structure is responsible for the different reactivity of both fractions of the DDGS char. A similarity could be expected for the first stage given the occurrence of the reaction process over approximately the same temperature range as for lignocellulosic chars. However, as already observed for the devolatilization stage, the ash most likely exerts a catalytic action on the activity of the heterogeneous reactions thus modifying the associated kinetic parameters.

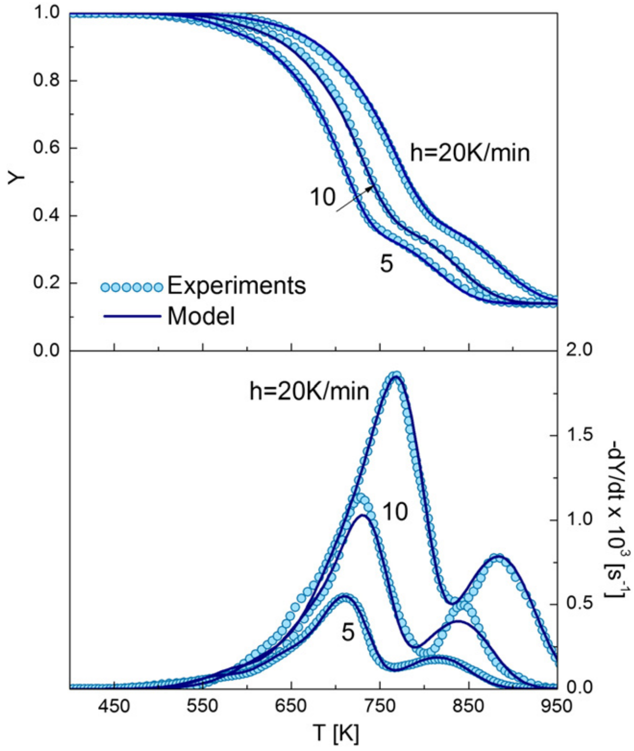

Fig. 6. Comparison between measured (symbols) and simulated (solid lines) thermogravimetric curves for the DDGS char samples at various heating rates, h, in air up to a temperature 950 K (kinetic parameters listed in Table 3).

4. Conclusions

The combustion behavior of DDGS and the corresponding char, obtained from pellets pyrolyzed at 800 K in an isothermal reactor, is investigated using a thermogravimetric system allowing for a precise control of the sample temperature. As expected, a zone of oxidative devolatilization is followed by the combustion of the charred residue. Both the shape of the rate curve and the temperature range where oxidative devolatilization of DDGS and combustion of char take place are highly different from those exhibited by wood. Conversion of DDGS takes place over a much wider temperature range (about 450–700 K) with slower rates. Although, for the most intense devolatilization zone, a shoulder and a peak can be identified their positions do not coincide with those exhibited by wood. The kinetic analysis, carried out using experimental data produced at various heating rates, reveals that the description of this reaction stage requires four reactions whose activation energies are much lower than those estimated for woody materials. It is plausible that the much lower percentages of the usual components of lignocellulosic materials and mainly the large presence of other classes of compounds (extractives, proteins and starch) and ashes in DDGS are responsible for such a behavior.

Contrary to lignocellulosic materials whose char exhibits a single well defined combustion peak, the DDGS char combustion occurs according to a two-step process with the second one displaced at much higher temperatures. As a consequence, the average combustion rates are slower. It can be hypothesized that the different chemical nature of the precursor gives rise to the formation of two char fractions with different reactivity. The kinetic evaluation indicates that two global reactions are sufficient to describe this stage but the activation energies are again lower than those usually reported for lignocellulosic chars, especially for the first reaction step. This result is plausibly associated with the large quantity of ash and its peculiar composition and the different morphological structure of the carbonaceous matrix.

Acknowledgments

This work is part of the activities carried out in the framework of the European “Biofuels Research Infrastructure for Sharing Knowledge (BRISK)” project (http://www.briskeu.com/), the partial support of which is gratefully acknowledged. The authors also thank Mr. Luciano Cortese (Istituto di Ricerche sulla Combustione, CNR, Napoli, Italy) for the SEM images of the samples.

References

[1] G. Eriksson, A. Grimm, N. Skoglund, D. Boström, M. Öhman, Combustion and fuel characterisation of wheat distillers dried grain with solubles (DDGS) and possible combustion applications, Fuel 102 (2012) 208–220.
[2] http://www.grains.org/index.php/buying-selling/ddgs-user-handbook.
[3] J. Giuntoli, Characterization of 2nd Generation Biomass Under Thermal Conversion and the Fate of Nitrogen, PhD Thesis Delft University of Technology, 2010, ISBN 978-90-9025803-4.
[4] C. Di Blasi, Combustion and gasification rates of lignocellulosic chars, Progress in Energy and Combustion Science 35 (2009) 121–140.
[5] C. Branca, C. Di Blasi, Global intrinsic kinetics of wood oxidation, Fuel 83 (2004) 81–87.
[6] G. Varhegyi, E. Meszaros, M.J. Antal, J. Bourke, E. Jakab, Combustion kinetics of corncob charcoal and partially demineralized corncob charcoal in the kinetic regime, Industrial & Engineering Chemistry Research 45 (2006) 4962–4970.
[7] G. Varhegyi, Aims and methods in non-isothermal reaction kinetics, Journal of Analytical and Applied Pyrolysis 79 (2007) 278–288.
[8] C. Branca, C. Di Blasi, Devolatilization and combustion kinetics of wood chars, Energy & Fuels 17 (2003) 1609–1615.

[9] J. Jauhiainen, J.A. Conesa, R. Font, I.M. Gullón, Kinetics of the pyrolysis and combustion of olive oil solid waste, Journal of Analytical and Applied Pyrolysis 72 (2004) 9–15.

[10] V. Leroy, D. Cancellieri, E. Leoni, Thermal degradation of ligno-cellulosic fuels: DSC and TGA studies, Thermochimica Acta 451 (2006) 131–138.

[11] C. Branca, A. Iannace, C. Di Blasi, Devolatilization and combustion kinetics of *Quercus cerris* bark, Energy & Fuels 21 (2007) 1078–1084.

[12] R. Font, J.A. Conesa, J. Molto, M. Munoz, Kinetics of pyrolysis and combustion of pine needles and cones, Journal of Analytical and Applied Pyrolysis 85 (2009) 276–286.

[13] G. Várhegyi, Z. Czégény, C. Liu, K. McAdam, Thermogravimetric analysis of tobacco combustion assuming DAEM devolatilization and empirical char-burnoff kinetics, Industrial & Engineering Chemistry Research 49 (2010) 1591–1599.

[14] J.A. Conesa, A. Domene, Biomasses pyrolysis and combustion kinetics through n-th order parallel reactions, Thermochimica Acta 523 (2011) 176–181.

[15] M. Brostrom, A. Nordin, L. Pommer, C. Branca, C. Di Blasi, Influence of torrefaction on the devolatilization and oxidation kinetics of wood, Journal of Analytical and Applied Pyrolysis 96 (2012) 100–109.

[16] A. Anca-Couce, N. Zobel, A. Berger, F. Behrendt, Smouldering of pine wood: kinetics and reaction heats, Combustion and Flame 159 (2012) 1708–1719.

[17] R. Abreu Naranjo, J.A. Conesa, E. Foppa Pedretti, O. Romero Romero, Kinetic analysis: simultaneous modeling of pyrolysis and combustion processes of *Dichrostachys cinerea*, Biomass and Bioenergy 36 (2012) 170–175.

[18] G. Várhegyi, Z. Sebestyen, Z. Czegeny, F. Lezsovits, S. Konczol, Combustion kinetics of biomass material in the kinetic regime, Energy & Fuels 26 (2012) 1323–1335.

[19] D. Tapasvi, R. Khalil, G. Várhegyi, Ø. Skreiberg, K. Tran, M. Grønli, Kinetic behavior of torrefied biomass in an oxidative environment, Energy & Fuels 27 (2013) 1050–1060.

[20] C. Branca, C. Di Blasi, A unified mechanism of the combustion reactions of lignocellulosic fuels, Thermochimica Acta 565 (2013) 58–64.

[21] C. Branca, C. Di Blasi, Oxidation kinetics of chars generated from the acid-catalyzed pyrolysis of corncobs, Fuel Processing Technology 123 (2014) 47–56.

[22] J. Giuntoli, W. de Jong, S. Arvelakis, H. Spliethoff, A.H.M. Verkooijen, Quantitative and kinetic TG-FTIR study of biomass residue pyrolysis: dry distiller's grains with solubles (DDGS) and chicken manure, Journal of Analytical and Applied Pyrolysis 85 (2009) 301–312.

[23] B. Gudka, L.I. Darvell, J.M. Jones, A. Williams, P.J. Kilgallon, N.J. Simms, R. Laryea-Goldsmith, Fuel characteristics of wheat-based Dried Distillers Grains and Solubles (DDGS) for thermal conversion in power plants, Fuel Processing Technology 94 (2012) 123–130.

[24] V. Pasangulapati, K.D. Ramachandriya, A. Kumar, M.R. Wilkins, C.L. Jones, R.L. Huhnke, Effects of cellulose, hemicellulose and lignin on thermochemical conversion characteristics of the selected biomass, Bioresource Technology 114 (2012) 663–669.

[25] L. Wang, A. Kumar, M.A. Hanna, C.L. Weller, D.D. Jones, Thermal degradation kinetics of distiller's grains and solubles in nitrogen and air, Energy Sources, Part A: Recovery, Utilization, and Environmental Effects 31 (2009) 797–806.

[26] L. Wang, A. Shahbazi, M.A. Hanna, Characterization of corn stover, distiller grains and cattle manure for thermochemical conversion, Biomass and Bioenergy 35 (2011) 171–178.

[27] X. Meng, W. de Jong, F.S. Badri, P. Benito, F. Basile, A.H.M. Verkooijen, Combustion study of partially gasified willow and DDGS chars using TG analysis and COMSOL modeling, Biomass and Bioenergy 39 (2012) 356–369.

[28] C.A. Mullen, A.A. Boateng, K.B. Hicks, N.M. Goldberg, R.A. Moreau, Analysis and comparison of bio-oil produced by fast pyrolysis from three barley biomass/byproduct streams, Energy & Fuels 24 (2010) 699–706.

[29] A. Sanna, S. Li, R. Linforth, K.A. Smart, J.M. Andrésen, Bio-oil and bio-char from low temperature pyrolysis of spent grains using activated alumina, Bioresource Technology 102 (2011) 10695–10703.

[30] A. Tavasoli, M.G. Ahangari, C. Soni, A.K. Dalai, Production of hydrogen and syngas via gasification of the corn and wheat dry distiller grains (DDGS) in a fixed-bed micro reactor, Fuel Processing Technology 90 (2009) 472–482.

[31] A. Kumar, K. Eskridge, D.D. Jones, M.A. Hanna, Steam–air fluidized bed gasification of distillers grains: Effects of steam to biomass ratio, equivalence ratio and gasification temperature, Bioresource Technology 100 (2009) 2062–2068.

[32] P. Piotrowska, M. Zevenhoven, M. Hupa, J. Giuntoli, W. de Jong, Residues from the production of biofuels for transportation: characterization and ash sintering tendency, Fuel Processing Technology 105 (2013) 37–45.

[33] C. Di Blasi, C. Branca, A. Galgano, Biomass screening for the production of furfural via thermal decomposition, Industrial & Engineering Chemistry Research 49 (2010) 2658–2671.

[34] Y. Kim, N.S. Mosier, R. Hendrickson, T. Ezeji, H. Blaschek, B. Dien, M. Cotta, B. Dale, M.R. Ladisch, Composition of corn dry-grind ethanol by-products: DDGS, wet cake, and thin stillage, Bioresource Technology 99 (2008) 5165–5176.

[35] M. Lanzetta, C. Di Blasi, F. Buonanno, An experimental investigation of heat transfer limitations in the flash pyrolysis of cellulose, Industrial & Engineering Chemistry Research 36 (1997) 542–552.

[36] C. Branca, C. Di Blasi, H. Horacek, Analysis of the combustion kinetics and the thermal behavior of an intumescent system, Industrial & Engineering Chemistry Research 41 (2002) 2104–2114.

[37] C. Branca, C. Di Blasi, A. Casu, V. Morone, C. Costa, Reaction kinetics and morphological changes of a rigid polyurethane foam during combustion, Thermochimica Acta 399 (2003) 127–137.

[38] C. Branca, C. Di Blasi, A multi-step mechanism for the devolatilization of biomass fast pyrolysis oils, Industrial & Engineering Chemistry Research 45 (2006) 5891–5899.

[39] C. Branca, C. Di Blasi, Combustion kinetics of secondary biomass chars in the kinetic regime, Energy & Fuels 24 (2010) 5741–5750.

[40] C. Branca, C. Di Blasi, Combustion kinetics of two core materials for sandwich structures, Journal of Thermal Analysis and Calorimetry 117 (2014) 961–972.

[41] C. Di Blasi, C. Branca, F. Masotta, E. De Biase, Experimental analysis of reaction heat effects during beech wood pyrolysis, Energy & Fuels 27 (2013) 2665–2674.

[42] C. Di Blasi, A. Galgano, C. Branca, Influences of the chemical state of alkaline compounds and the nature of alkali metal on wood pyrolysis, Industrial & Engineering Chemistry Research 48 (2009) 3359–3369.

[43] S. Nair, M. Knoblauch, S. Ullrich, B.K. Baik, Microstructure of hard and soft kernels of barley, Journal of Cereal Science 54 (2011) 354–362.

[44] http://www.healthbanquet.com/wheatgrass-life-cycle.html.

[45] C. Branca, C. Di Blasi, Parallel- and series-reaction mechanisms of wood and char combustion, Thermal Science 8 (2004) 51–63.